Biochemical Pharmacology 82 (2011) 1663–1672

Contents lists available at SciVerse ScienceDirect

Biochemical Pharmacology

journal homepage: www.elsevier.com/locate/biochempharm

Lovastatin inhibits proliferation of anaplastic thyroid cancer cells through up-regulation of p27 by interfering with the Rho/ROCK-mediated pathway

Wen-Bin Zhong [a], Sung-Po Hsu [b], Pei-Yin Ho [b], Yu-Chih Liang [c], Tien-Chun Chang [d], Wen-Sen Lee [a,b,e,*]

[a] Department of Physiology, Medical College, Taipei Medical University, Taipei 110, Taiwan
[b] Graduate Institutes of Medical Sciences, Medical College, Taipei Medical University, Taipei 110, Taiwan
[c] Department of Biomedical Technology, Medical College, Taipei Medical University, Taipei 110, Taiwan
[d] Division of Endocrinology, Department of Internal Medicine, National Taiwan University Hospital, College of Medicine, National Taiwan University, Taipei 100, Taiwan
[e] Cancer Research Center, Taipei Medical University Hospital, Taipei, Taiwan

ARTICLE INFO

Article history:
Received 1 July 2011
Accepted 24 August 2011
Available online 2 September 2011

Keywords:
Anaplastic thyroid cancer
HMG-CoA reductase
Lovastatin
p27
Rho

ABSTRACT

Previously, we demonstrated that lovastatin, a HMG-CoA reductase inhibitor, induced apoptosis, differentiation, and inhibition of invasiveness of human anaplastic thyroid carcinoma cells (ATCs). Here, we further examined the effect of lovastatin on the growth of ARO cells. Lovastatin (0–20 μM) concentration-dependently decreased cell number in cultured ATC and arrested the cell at the G0/G1 phase of the cell cycle. Western blot analysis revealed that lovastatin caused an increase of the protein level of p27 and cyclin-dependent kinase (CDK)4 and a decrease of the protein level of cyclin A2, cyclin D3, and phosphorylated Rb (pRb), but did not significantly change the protein levels of p21, cyclins D1 and E, and CDK2, in ARO cells. The formation of the CDK2–p27 complex was increased and the CDK2 activity was decreased in the lovastatin-treated ARO cells. Pretreatment of ARO cells with a p27, but not p21, antisense oligonucleotide prevented the lovastatin-induced G0/G1 arrest in ARO cells. The lovastatin-induced growth inhibition and translocation of RhoA and Rac1 in ARO cells were completely prevented by mevalonate and partially by geranylgeranyl pyrophosphate. Treatment of ARO cells with Y27632, an inhibitor of Rho-associated kinase, abolished the GGPP-mediated prevention of lovastatin-induced anti-proliferation and up-regulation and prolonged degradation of p27. Taken together, these data suggest that lovastatin treatment caused a reduction of Rho geranylgeranylation, which in turn increased the expression and stability of p27, and then inhibited ARO cell proliferation. These data suggest that lovastatin merits further investigation as multipotent therapy for treatment ATC.

© 2011 Elsevier Inc. All rights reserved.

1. Introduction

It has been shown that malignant thyroid cancers are developed through a dedifferentiation transformational process from benign thyroid tumors such as papillary and follicular thyroid tumors with well-differentiated characteristics [1,2]. Patients with papillary or follicular thyroid tumors are generally treated with thyroidectomy and ^{131}I-activated radiotherapy. Patients, who received this treatment regimen, use to have a good prognosis (85% of these patients survive more than 5 years) [3,4]. However, 15% of these patients might develop malignant cancers, such as poorly differentiated papillary and anaplastic thyroid cancers (ATCs). ATC is one of the most aggressive malignant tumors. Patients with ATC have a poor prognosis with a mean survival time of 2–6 months due to an aggressiveness of proliferation and invasive and metastatic outgrowth. Surgery, radiotherapy, and chemotherapy are not helpful in improving the survival time and the life quality of such patients [2].

Statins, HMG-CoA reductase inhibitors, are the frequently prescribed drugs for treating hypercholesterolemia and related cardiovascular diseases [5–7]. Recent *in vitro* and *in vivo* studies have shown the potential applications of statins in cancer therapy [8]. Lovastatin, an inhibitor of HMG-CoA reductase which converts HMG-CoA to mevalonate, is the first generation of statin drugs for lowering plasma cholesterol. In addition to decreasing blood cholesterol, inhibition of mevalonate synthesis leads to a depletion of its downstream nonsterol isoprenoids, such as farnesyl-pyrophosphate (FPP), and geranylgeranyl-pyrophosphate (GGPP) [9,10]. Isoprenoid intermediates function as lipid moieties for the post-translational modifications of a number of proteins such as Ras and Rho small GTPases. Membrane translocation is crucial to activate both Ras and Rho families by post-translational prenylation [11,12]. Inhibition of farnesylation and geranylgeranylation causes an inactivation of Ras and Rho.

* Corresponding author at: Graduate Institute of Medical Sciences, Ant, Taipei Medical University, 250 Wu-Hsing Street, Taipei 110, Taiwan.
Tel.: +886 2 27361661x3420; fax: +886 2 23778620.
E-mail address: wslee@tmu.edu.tw (W.-S. Lee).

0006-2952/$ – see front matter © 2011 Elsevier Inc. All rights reserved.
doi:10.1016/j.bcp.2011.08.021

Since ATC is resistant to conventional chemotherapy and thus ultimately lethal, a novel therapeutic approach has been devised using drugs that stimulate cellular differentiation, combined with extirpation of cancerous areas by radioiodine (I^{131}) or surgical means [13]. Recently, we demonstrated that a higher concentration of lovastatin (100 μM) was able to induce apoptotic cell death of ARO by activation of mitochondria-mediated caspase cascade *in vitro* [14,15]. ARO cells used in the present study are representative of the typical ATC cells with hyperproliferative and chemoresistant features. Here, we demonstrated that lovastatin at lower concentrations exerted an anti-proliferation effect on human ATC cells through increases of p27 mediated by the reduction of Rho geranylgeranylation.

2. Materials and methods

2.1. Chemicals and antibodies

Lovastatin was a gift from Standard Chemical and Pharmacy Co. (Taipei, Taiwan). Fetal bovine serum (FBS), culture medium RPMI 1640, penicillin and streptomycin were obtained from Life Technologies/Gibco (Grand Island, NY). Y27632 was purchased from Tocris Bioscience (Ellisville, MO). Bovine serum albumin (BSA), mevalonate, GGPP, FPP, and gelatin were purchased from Sigma–Ardrich (St. Louis, MO). Antibody against pan-Ras was purchased from Millipore/Upstate (Billerica, MA). Antibodies against RhoA, Rac1, α-tubulin, cyclins, cyclin-dependent kinases (CDKs), and phosphor-Rb were purchased from Santa Cruz Biotechnology (Santa Cruz, CA). Antibodies against E-cadherin, p21, and p27 were obtained from BD Transduction Laboratories (San Diego, CA), and anti-GAPDH antibody was purchased from Jackson ImmunoResearch Laboratories (West Grove, PA).

2.2. Cell culture

The human anaplastic thyroid cancers (ARO, 8305C, SW1736, and KAT4B) were cultured in RPMI 1640 medium supplemented with 5% FBS and antibiotics (100 U/mL penicillin and 100 μg/mL streptomycin) at 37 °C in CO_2 incubator. For study cell growth inhibition, ATC cells (1×10^6 cells/mL) were seeded onto 24-well plates and then cultured overnight allowing cell attachment, followed by treatment with lovastatin at various concentrations as indicated for 48 h. At the end of experiment, cells were collected for number counting or phase analysis of cell cycle. To analyze the levels of mRNA and protein of p21 and p27, ARO cells were co-treated with isoprenoids (such as mevalonate, GGPP, and FPP) or Y27632 with lovastatin for 12–48 h.

2.3. Cell proliferation assay

ATC cells were seeded onto 24-well plate (1×10^6 cells/mL per well) and cultured overnight. The cells were then treated with various concentrations (5–20 μM) of lovastatin for 48 h. In some experiments, cells were co-treated with lovastatin (20 μM) and isoprenoids (such as mevalonate, FPP, and GGPP), and then incubated for 24–48 h at 37 °C. At the end of the experiment, adherent cells were collected and counted with a hemocytometer. In the experiments of cells co-treated with lovastatin and Y27632, cell proliferation was examined by MTT [3-(4,5-methylthiazol-2-yl)-2,5-diphenyl-tetrazolium bromide] assay. Cells were plated at a density of 1×10^6 cells/well in 24-well plates, allowed to adhere overnight, and then treated with lovastatin for 48 h. After incubation, 400 μg/mL MTT solution was added and incubated for 1 h. The medium was then aspirated, and the dark blue crystal product extracted with DMSO. Colorimetric change was read on a microtiter plate reader with a 570 nm filter and a reference wavelength 430 nm.

2.4. Fluorescence-activated cell sorting (FACS) analysis of cell cycle

The cell distribution at each phase of the cell cycle was assessed according to the percentage of cells with the content of DNA using the propidium iodide (PI)-staining technique. Briefly, the treated cells were washed with PBS, centrifuged at $1000 \times g$ for 3 min, fixed with ethanol, and stored overnight at −20 °C. On the following day, they were washed with PBS, and then incubated with PBS containing 1 mg/mL RNase A (Sigma) at 37 °C for 30 min and 50 μg/mL PI (Sigma) at room temperature in the dark for 1 h. Cell cycle phases of stained cells were acquired using FACSCalibur flow cytometer (Becton Dickinson, San Jose, CA) and further analyzed using the CELLQuest software.

2.5. Transfection of cells with antisense oligonucleotides

The p21- and p27-specific antisense (AS) oligonucleotide phosphothioates (S-oligos) sequence used in the experiments are p21AS: 5′-TCTTCTGTTCTGTTGGCCCT-3′; p27AS: 5′-UCCGCGCC-CAGCUCC-3′ [16]. They were synthesized and purified using high-performance liquid chromatography by Sigma-Genosys, Inc. (Houston, TX). For knock-down of p21 and p27, ARO cells (3×10^6 cells/well) were cultured in 6-well plates overnight followed by transfection with AS S-oligos of p27 or p21. Transfection of S-oligo (50 nM) with TransfectAMINE Plus reagent (Invitrogen) was performed following instructions of the manufacturer.

2.6. Separation of particulate and cytosolic fractions

Separation of cytosolic and particulate fractions was performed as described previously [16]. Briefly, the cells were washed with cold PBS and lysed by 5-cycle freeze–thawing in Hepes buffer [50 mM HEPES (pH 7.5), 50 mM NaCl, 2 mM EDTA, 1 mM $MgCl_2$, 10 mM NaF, 1 mM DTT, 10 mg/mL leupeptin, 10 mg/mL aprotinin, and 1 mM phenylmethylsulfonyl fluoride (PMSF)], and centrifuged at $100{,}000 \times g$ for 30 min at 4 °C. The supernatant was collected as the cytosolic fraction. Pellets were washed with Hepes buffer, homogenized in the lysis buffer containing 2% Triton X-100 plus 1% SDS, and then centrifuged at $10{,}000 \times g$ for 30 min at 4 °C. The supernatant was then collected as the particulate (membrane) fraction.

2.7. Immunoprecipitation and kinase activity assay

Cells were lysed in lysis buffer (137 mM NaCl, 20 mM Tris, pH 7.9, 10 mM NaF, 5 mM EDTA, 1 mM EGTA, 10% (v/v) glycerol, 1% Triton X-100, 1 mM sodium orthovanadate, 1 mM sodium pyrophosphate, 100 μM β-glycerophosphate, 1 mM PMSF, 10 μg/mL aprotinin, 10 μg/mL leupeptin). For pull-down of p27, cell lysates (500 μg) were incubated with anti-p27 antibody and protein A/G PLUS-agarose (Santa Cruz Biotechnology) was added during the last 2 h of incubation. Immunoprecipitates were washed five times with lysis buffer, and then resuspended in 3× Laemmli sample buffer with 50 mM dithiothreitol. For immunoblotting analysis, 40 μg of proteins was separated by 12% SDS-PAGE and transferred to polyvinylidine difluoride (PVDF) membranes (GE Healthcare Life Science, Piscataway, NJ). Membranes were incubated with anti-p27, anti-Skp2, and anti-ubiquitin antibodies followed by horseradish peroxidase-conjugated secondary antibodies (Jackson ImmunoResearch Laboratories, West Grove, PA) for ECL detection (GE Healthcare Life Science). For the CDK2 and CDK4 kinase activity assay, cell lysates were incubated with anti-CDK2 or anti-CDK4 antibody (2 μg/mL) and protein A coated sepharose beads (GE Healthcare Life Science). The

immunoprecipitants were washed five times with lysis buffer, and once with kinase assay buffer (25 mM Hepes pH 7.4, 25 mM $MgCl_2$, 25 mM glycerolphosphate, 1 nM orthovanadate, 2 mM DTT). The phosphorylation levels of histone H1 (for CDK2 activity) and Rb-glutathione S-transferase (GST) fusion protein (for CDK4 activity) were detected by incubating the immunocomplex beads with 40 μL of hot kinase solution [0.25 μL (2 μg) of Rb-GST fusion protein (Santa Cruz Biotechnology), 0.5 μL of (γ-^{32}P) ATP (GE Healthcare Life Science), 0.5 μL of 0.1 mM ATP and 38.75 μL of kinase buffer] at 37 °C for 30 min, and then stopped by boiling the samples in SDS sample buffer (120 mM Tris–Cl, pH 6.8, 2% SDS, 10% glycerol, 5% β-mercaptoethanol, 0.25% bromphenol blue) for 5 min. The samples were analyzed by 12% SDS-PAGE, and the gel was then dried for autoradiography. For elucidating proteins associated with CDK2, immunoprecipitants were washed 3 times followed by re-suspending in the reducing SDS loading buffer, and subsequently subjected to Western blot for analysis of the protein–protein associations of p27 or p21 with CDK2.

2.8. Western blot analysis

Total protein extracts were subjected to electrophoresis on 12% polyacrylamide gels, and then transferred (350 mA, 2 h) to Hybond^{TM}-P polyvinylidine difluoride (PVDF) membranes (Jackson ImmunoResearch Laboratories). The membrane was probed with specific primary antibodies in 1% BSA/TBST, washed with TBST (3 × 10 min), and then incubated with the HRP-conjugated secondary antibody. Target proteins were observed using the enhanced chemiluminescence (ECL) detection system (GE Healthcare Life Science) and Fuji super RX film (Fuji photo film Co., Tokyo, Japan).

2.9. Statistical analysis

All data were expressed as the mean value ± S.E.M. Comparisons were subjected to Student's two-tailed *t*-test. Significance was accepted at $p < 0.05$.

3. Results

3.1. Inhibition of cell proliferation in lovastatin-treated ATC

To study the anti-proliferative effect of lovastatin, ATC were treated with various concentrations of lovastatin (5–20 μM) for 48 h. The cells were then harvested and counted using trypan blue exclusion method. As shown in Fig. 1A, lovastatin decreased ARO cell number in a concentration-dependent manner. To confirm the anti-proliferative effect of lovastatin on ARO cells, FACS analysis of cell cycle was conducted. Lovastatin (20 μM) induced a significant accumulation of cells at the G1 phase of the cell cycle (Fig. 1B). The anti-proliferation effect of lovastatin was also observed in three other ATC cell lines, 8305C, SW1736 and KAT4B (Fig. 2A and B).

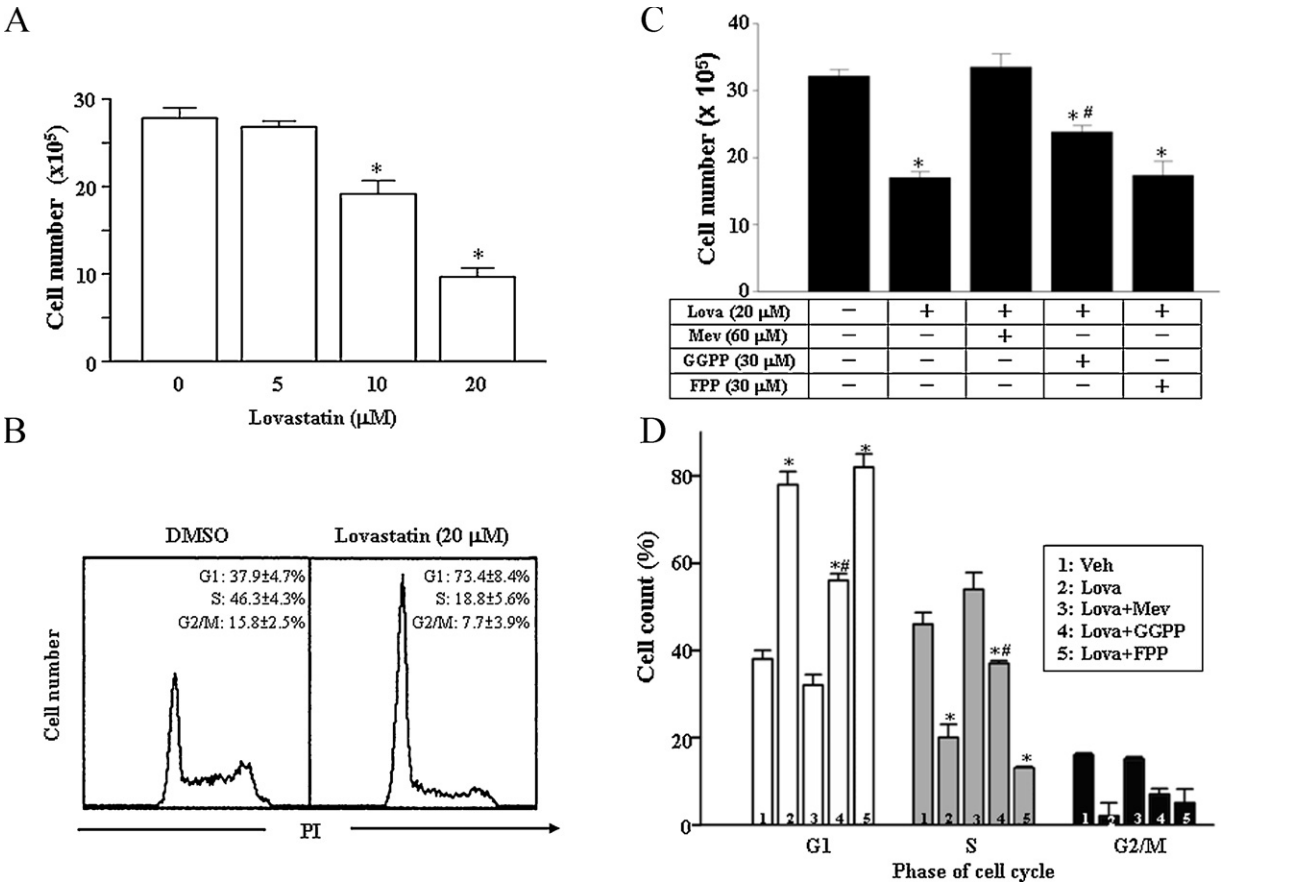

Fig. 1. Inhibitory effects of lovastatin on ARO cell growth. ARO cells (10^6 cells/mL, per well) were seeded into 24-well plates, and then treated with lovastatin (0–20 μM) for 48 h. (A) Lovastatin (5–20 μM) concentration-dependently inhibited the number of ARO cells. Cell number was counted using trypan blue exclusion method. Values represent the means ± S.E.M. ($n = 3$). *$p < 0.05$ vs. control (DMSO without lovastatin). (B) FACS analysis of DNA content was performed at 48 h after release from quiescence by incubating the cells in culture media supplemented with 10% FBS and 0.1% DMSO without (left panel) or with 20 μM lovastatin (right panel). Results from a representative experiment ($n = 4$) are shown. Percentage of cells at the G1, S, or G2/M phase of the cell cycle was determined using established CellFIT DNA analysis software. The lovastatin-induced decreases of cell number (C) and G1 cell cycle arrest (D) in ARO were completely prevented by mevalonate and partially by GGPP, but not by FPP. The ARO cells (10^6 cells/well) were treated with lovastatin with or without isoprenoids (such as 60 μM mevalonate, 30 μM GGPP, or 30 μM FPP), and then incubated for 48 h. Values represent the means ± S.E.M. ($n = 3$). Significance was accepted at $p < 0.05$. *Different from control group. #Different from lovastatin-treated group. Lov, lovastatin; Mev, mevalonate.

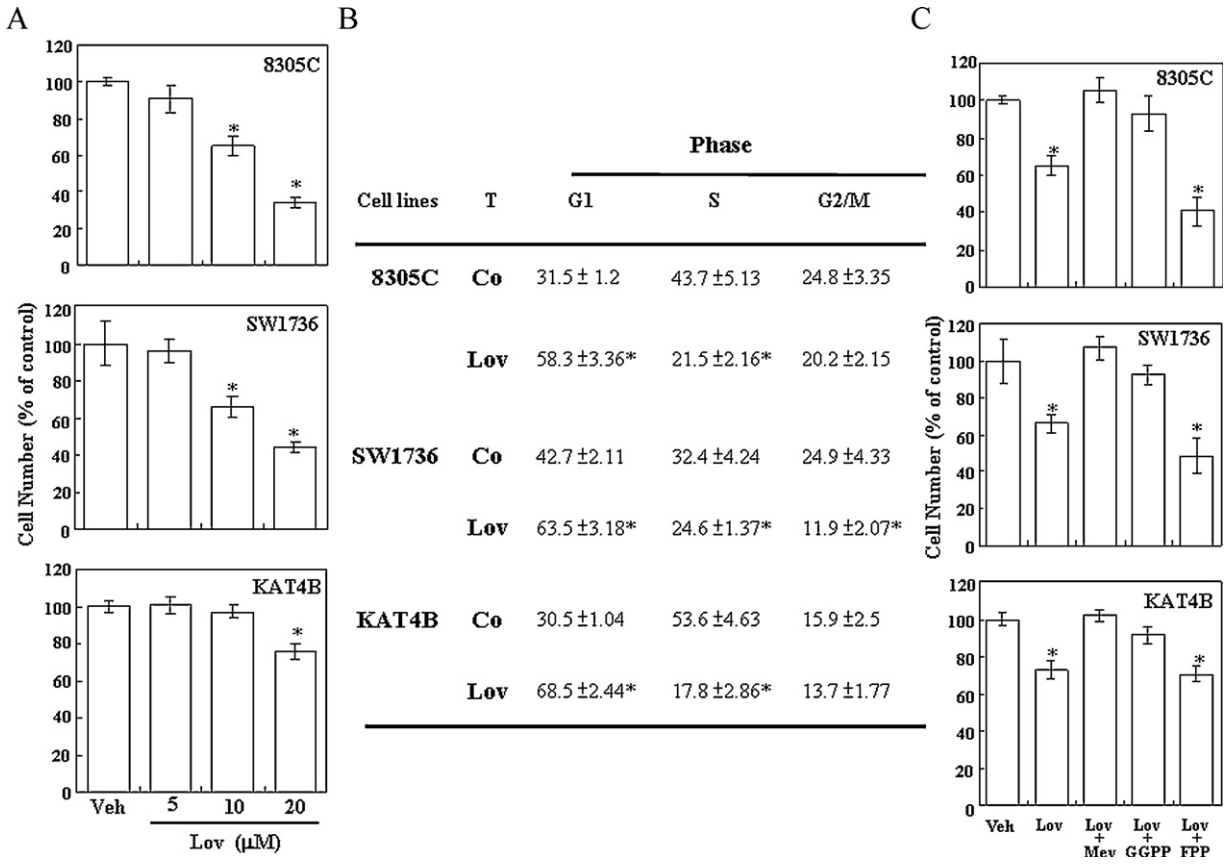

Fig. 2. Inhibitory effects of lovastatin on ATC cell growth. (A) Lovastatin (5–20 μM) concentration-dependently inhibited the growth of 8305C, SW1736 and KAT4B cells. (B) Lovastatin-induced cell cycle arrest of 8305C, SW1736 and KAT4B cells at the G1 phase. (C) The lovastatin-induced growth inhibition was completely prevented by mevalonate and GGPP, but not by FPP. The ATC cells (10^6 cells/well) were treated with lovastatin (10 μM for 8305C and SW1736 and 20 μM for KAT4B) with or without isoprenoids (such as 60 μM mevalonate, 30 μM GGPP, or 30 μM FPP), and then incubated for 48 h. Values represent the means ± S.E.M. ($n = 3$). Significance was accepted at $p < 0.05$. *Different from control group. Lov, lovastatin; Mev, mevalonate.

Apoptotic cell death (cells with hypodiploid DNA) was not observed in this treatment, suggesting that the growth inhibition induced by lovastatin was due to an arrest of DNA replication.

3.2. Mevalonate and GGPP prevents the lovastatin-induced growth inhibition

Lovastatin inhibits the conversion of HMG-CoA to mevalonate, which is a precursor of isoprenoid metabolites (such as isopentenyl-pp, FPP, and GGPP) in the cholesterol biosynthetic pathway. To examine whether the reduction of mevalonate formation is involved in the anti-proliferation effect caused by lovastatin, ATC cells (10×10^5/well) were co-treated with lovastatin and mevalonate for 48 h. As illustrated in Fig. 1C, mevalonate (60 μM) pretreatment abolished the lovastatin-induced growth suppression in ARO cells, whereas GGPP (30 μM) had partial effect and FPP (30 μM) had no significant effect. These findings were confirmed by cell cycle analysis (Fig. 1D). The lovastatin-induced cell accumulation at the G1 phase was completely prevented by mevalonate and partially by GGPP, but not by FPP. A similar finding was also observed in three other ATC cell lines, 8305C, SW1736 and KAT4B (Fig. 2C). These findings suggest that lovastatin-induced cell growth arrest via the depletion of intracellular mevalonate and its downstream isoprenyl metabolite GGPP, but not FPP.

3.3. Lovastatin inhibits membrane translocation of the Rho family

Post-translational prenylation is a unique modification for membrane translocation of Ras and Rho families. In addition, membrane anchorage of Ras and Rho family is essential for their functions. To determine whether associations of Ras and Rho protein with cellular membrane are altered by lovastatin, the protein levels of RhoA and Rac1 in particulate fraction were examined. The protein levels of RhoA and Rac1 were decreased by 55% and 65%, respectively, in particulate fractions of the lovastatin-treated ARO cells (Fig. 3A). These lovastatin-induced effects were prevented by co-treatment of the cells with mevalonate and GGPP, but not FPP. The level of particulate bound Ras protein was not significantly affected by these treatments. The absence of GAPDH in the membrane fraction ruled out the possible contamination from the cytosolic fraction. To further delineate the mechanisms by which the membrane translocation of Rho proteins was reduced, the post-translational modifications of Rho proteins were verified with Western blotting analysis (Fig. 3B), and ratios of unprocessed to processed proteins (Rho and Ras) were expressed with relative quantification (Fig. 3C). In ARO cells, protein processing of RhoA was inhibited by lovastatin. However, mevalonate and GGPP abolished the inhibitory effects of lovastatin on RhoA protein modification. In contrast, the processing of Ras protein was not affected significantly by lovastatin in the presence or absence of isoprenoids. To confirm that the lack of Ras responsiveness to lovastatin in ARO cells was not due to technical problems, the same experiment was conducted in the human umbilical vein endothelial cells (HUVEC). As shown in Fig. 3B and C (lower panels), the processing of Ras protein in HUVEC was inhibited by lovastatin. Moreover, the lovastatin-inhibited modifications of Ras protein in HUVEC were significantly prevented by mevalonate and FPP, but not by GGPP.

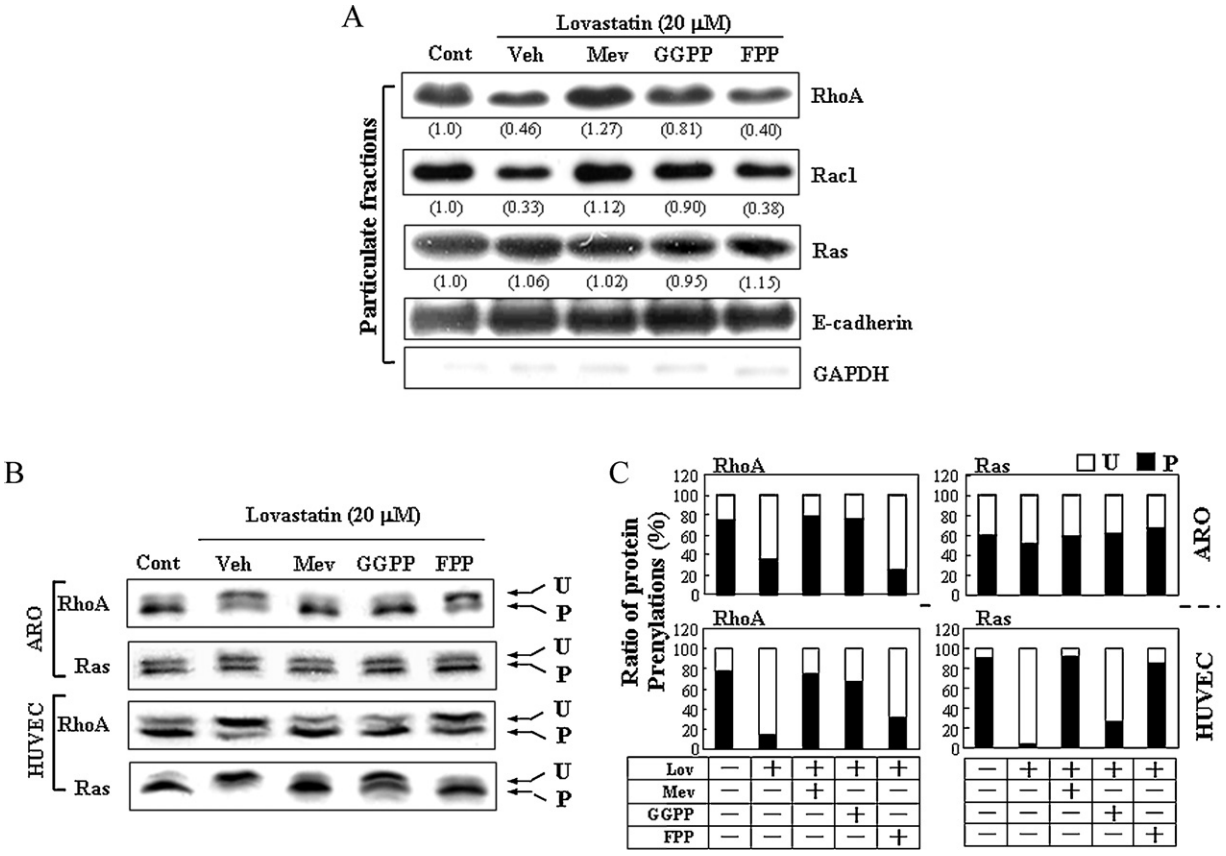

Fig. 3. Effects of lovastatin and isoprenoids on membrane translocation of Rho in ARO cells. (A) Lovastatin induced decreases of membrane translocation of Rho A and Rac 1, but not Ras. This inhibition was prevented completely by mevalonate and partially by GGPP, but not by FPP. ARO cells were co-treated with lovastatin and isoprenoids (mevalonate, GGPP, or FPP) for 48 h. The membrane translocation of Ras was not affected by lovastain. To confirm the purities of isolation, E-cadherin and GAPDH were used as a particulate (membranous) and cytosolic protein marker, respectively. Values shown in parentheses represent the quantified results after adjusted with their own E-cadherin levels. (B) Lovastatin inhibited the prenyl process of RhoA in ARO and HUVEC. The inhibitory effect of lovastatin on the prenyl process of Ras was only observed in HUVEC, but not in ARO (P, processed; U, unprocessed). (C) The ratios of the protein prenylation of RhoA and Ras were quantified by densitometric analysis. White bar, the isoprenyl processing status of Ras and RhoA was detected with 17% SDS-PAGE. Representative data from three independent experiments are shown. Cont, control (vehicle only); Mev, mevalonate; Lov, lovastatin.

3.4. Alterations of cell cycle activity in lovastatin-treated ARO cells

To further investigate the molecular mechanisms underlying lovastatin-induced G1 arrest, ARO cells were treated with lovastatin for 48 h, and then harvested for protein extraction and Western blot analysis. As illustrated in Fig. 4A, lovastatin (20 μM) decreased the level of cyclin A, cyclin D3, and pRb protein and increased the level of CDK4 protein, but did not significantly affect the levels of cyclin D1, cyclin E, and CDK2 protein in ARO cells. Since the CDK activity can be negatively regulated by CKIs, the levels of p21 and p27 protein were thus assayed in the lovastatin-treated ARO cells. Lovastatin (5–20 μM) concentration-dependently increased the protein levels of p27, but not p21, in ARO cells (Fig. 4B). The lovastatin-induced increases of p27 protein level were prevented by mevalonate and GGPP, but not by FPP (Fig. 4C).

3.5. Inhibition of the CDK2 activity by lovastatin

CKIs have been shown to inhibit the kinase activity of CDKs through direct association with the cyclin/CDK complex. Accordingly, we further conducted pull-down assay to examine the effect of lovastatin on the interaction between CDK and CKI. In the lovastatin-treated ARO, the formation of the CDK2–p27 complex, but not CDK2–p21 complex, was increased (Fig. 5A). To examine whether the increased CDK2–p27 complex is associated with the inhibition of CDK activation, which is necessary for cell cycle progression from the G_1 to S phase, the CDK activity was detected using autoradiography of the specific CDK substrate protein. As shown in Fig. 5B, the CDK2 activity was decreased by 30% in the lovastatin-treated cells. In addition, lovastatin-induced increases in CDK2–p27 association and decreases in the CDK2 activity were prevented by co-treatment of the cells with mevalonate and GGPP, but not FPP, suggesting that inhibition of GGPP/Rho/p27/CDK2 pathway is involved in the lovastatin-induced anti-proliferation effects on ATC cells. In contrast, the CDK4 kinase activity in the lovastatin-treated ARO was increased and this increased CDK4 activity was prevented by mevalonate and GGPP, but not by FPP.

3.6. Inhibition of RhoA/ROCK signaling pathway increases the expression and protein stability of p27

To examine whether transcription modulation is involved in the lovastatin-induced increases of p27 protein level, RT-PCR analysis was conducted. As illustrated in Fig. 6A, an increase of the level of p27 mRNA was observed at 2 h after lovastatin treatment and lasted for 48 h. Experiments were further conducted to examine whether RhoA is involved in the lovastatin-induced up-regulation of p27. As shown in Fig. 6B, both lovastatin and RhoA-DN apparently elevated expression of p27 transcripts, but not of p21. To examine further whether the stability of p27 protein contributes to the increase of p27 protein caused by lovastatin treatment, the degradation of p27 protein was examined following treatment with cycloheximide (CHX). ARO cells were treated with lovastatin

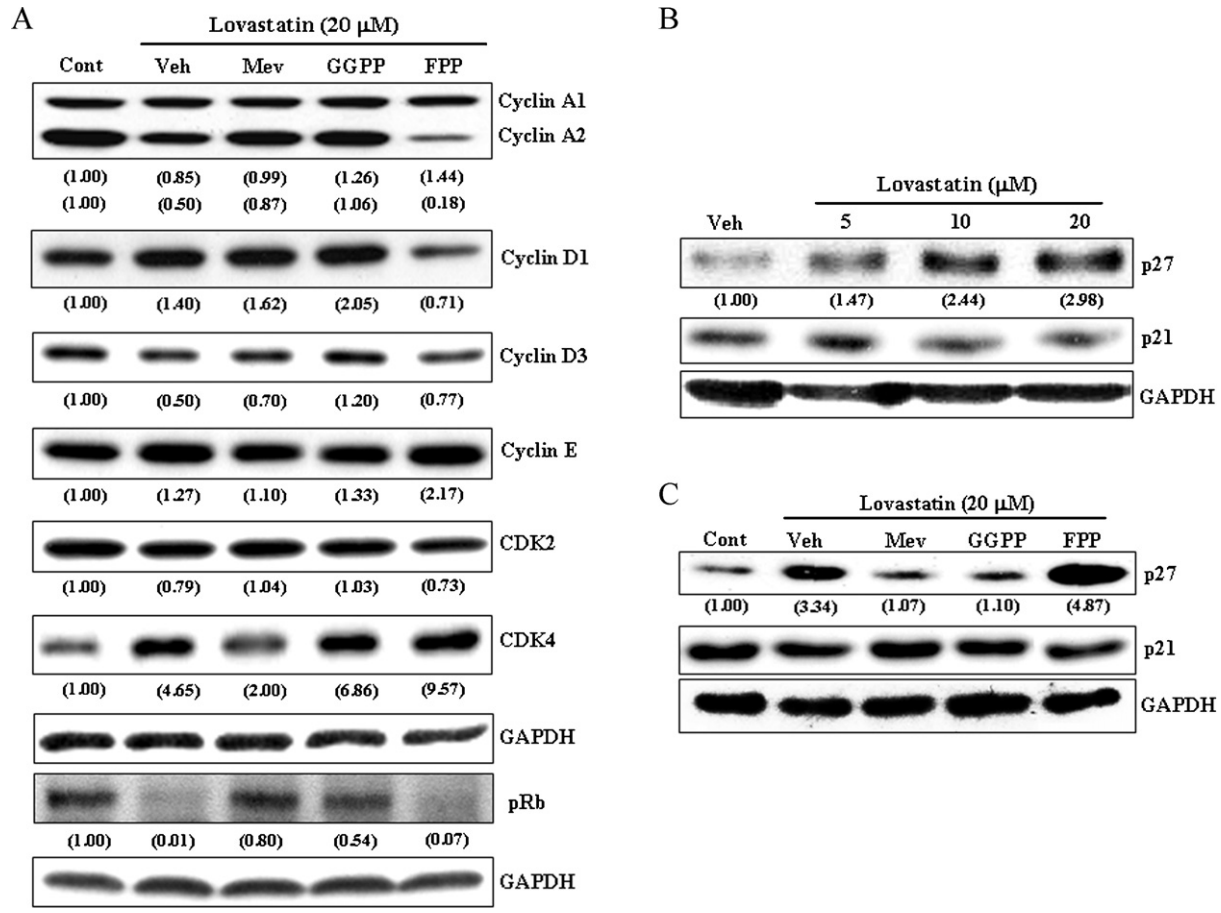

Fig. 4. Effects of lovastatin and isoprenoids on the protein levels of cyclins, CDKs, and CKIs. (A) Lovastatin decreased the level of cyclin A, cyclin D3, and pRb protein, increased the level of CDK4 protein, but did not affect significantly on the protein levels of cyclin D1, cyclin E, and CDK2. Results from a representative experiment are shown. Values shown in parentheses represent the quantified results after adjusted with their own GAPHD levels. (B) Lovastatin (5–20 μM) concentration-dependently increased the protein levels of p27, but not p21. Values shown in parentheses represent the relative protein abundance of p27, which has been normalized with corresponding GAPDH. (C) The lovastatin-induced increases of p27 protein were prevented by mevalonate and GGPP, but not FPP. Proteins were extracted from the cultured ARO at 48 h after treatment with lovastatin (20 μM) with or without isoprenoids (mevalonate, GGPP, or FPP), and then probed with proper dilutions of specific antibodies. Membrane was also probed with anti-GAPHD antibody to verify equivalent loading. Values shown in parentheses represent the relative protein abundance of p27, which has been normalized with corresponding GAPDH. CDK, cyclin-dependent kinase; CKI, CDK inhibitor.

or Y27632, a selective inhibitor of ROCK, for 48 h followed by CHX for 0.5 to 8 h. As illustrated in Fig. 7A, both lovastatin (20 μM) and Y27632 (2 μM) delayed the degradation of p27 protein. Fig. 7B shows that the half-life of p27 protein was prolonged by lovastatin and Y27632 for 12.8 and 6 folds, respectively. To examine whether suppression of the ubiquitination pathway is involved in the control of p27 protein stability, the experiment illustrated in Fig. 7C was carried out. In the presence of lovastatin, the formation of p27–Skp2 complex and the levels of ubiquitinated p27 and p27-associated proteins in ARO cells were decreased. These effects were prevented by pretreatment of the cell with GGPP (Fig. 7C). These results suggest that lovastatin increased the levels of p27 protein through increases of transcription and protein stability by inhibiting the RhoA/ROCK signaling-mediated pathway and the ubiquitination pathway.

3.7. Involvement of RhoA/ROCK in the lovastatin-induced anti-proliferation in ARO cells

To examine whether the RhoA/ROCK signaling pathway is involved in the lovastatin-induced antiproliferation, ARO cells were pretreated with Y27632 (2 μM) followed by lovastatin with or without GGPP. Pretreatment of ARO with GGPP prevented both p27 induction (Fig. 8A) and the growth inhibition (Fig. 8B) induced by lovastatin. However, these GGPP-induced prevention effects were abolished by Y27632 treatment. Treatment with Y-27632 alone also increased the levels of p27 protein with a 25% suppression of cell growth. To further confirm the role of p27 in lovastatin-induced G1 cell-cycle arrest, selective antisense oligonucleotides (AS) were used to knock-down either p27 or p21 (Fig. 8C). As shown in Fig. 8D, the lovastatin-induced G1-arrest was prevented by pretreatment with p27 AS, but not p21AS. These results suggest that lovastatin inhibited the proliferation of ARO cells through increasing the level of p27 protein.

4. Discussion

HMG-CoA reductase inhibitors have been widely used for treatment of hyperlipidemia and for reduction of cardiovascular morbidity and mortality of patients with hyperlipidemia [5,6]. In addition to the marked beneficial effects on lipid profile, HMG-CoA reductase inhibitors also have effects unrelated to reduction of cholesterol. Recent *in vitro* and *in vivo* studies have shown that statins exert an anti-cancer activity in various cancer cells [7,17,18]. However, the anti-cancer effects of statins on ATC, the most aggressively malignant thyroid cancer, have not been well investigated. Previously, our *in vitro* studies demonstrated that lovastatin is able to induce apoptotic cell death and to inhibit the invasiveness of ATC cells [14,16]. Moreover, induction of thyrocyte differentiation was observed in the poorly differentiated ARO cells

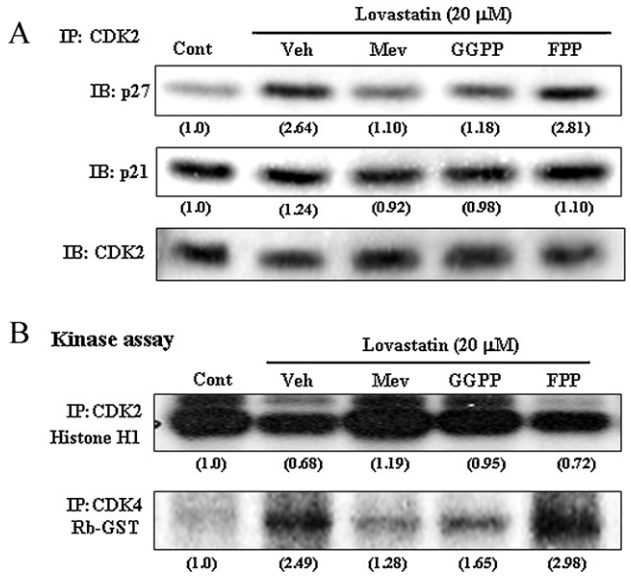

Fig. 5. Effects of lovastatin on the formation of CKI–CDK complex and CDK kinase activity. (A) Lovastatin increased the formation of CDK2–p27, but not CDK2–p21, complex in ARO cells. The lovastatin-induced increase in the formation of CDK2–p27 complex was prevented completely by mevalonate and partially by GGPP, but not by FPP. ARO cells were treated with lovastatin (20 μM) with or without isoprenoids (mevalonate, GGPP, or FPP) for 48 h. CDK2 was immunoprecipitated by anti-CDK2 antibody, and the CDK2–p21 and CDK2–p27 association were detected by anti-p21 antibody and anti-p27 antibody, respectively. Values shown in parentheses represent relative protein abundance of p27 and p21 associated with CDK2. (B) Treatment of ARO cells with lovastatin (20 μM) caused a reduction in the assayable CDK2 activity and an increase in the assayable CDK4 kinase activity. The lovastatin-induced decrease in the CDK2 activity and increase in the CDK4 activity were completely prevented by mevalonate and partially by GGPP, but not by FPP. Results from a representative experiment are shown. Values shown in parentheses represent relative phosphorylation levels of CDK substrates. IP, immunoprecipitation; IB: immunoblotting; CDK, cyclin-dependent kinase; CKI, CDK inhibitor.

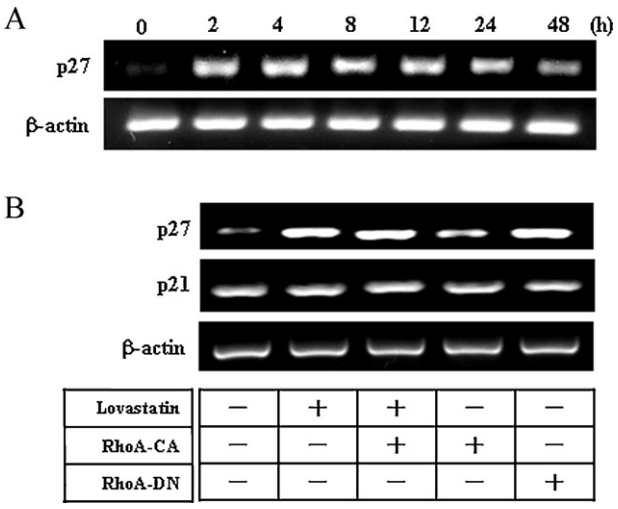

Fig. 6. Effects of RhoA on p27 transcriptional induction by lovastatin. (A) Lovastatin (20 μM) increases the levels of p27 mRNA in ARO cells. RT-PCR products of β-actin were used as an internal control. (B) Inhibition of RhoA was required for lovastatin-increased p27 mRNA expression. ARO plated in a 12-well plate were subjected to transfection with constitutive active (RhoA-CA) or dominant negative (RhoA-DN) mutants by liposome method. After incubation for 24 h, the cell was treated with or without lovastatin for 8 h, and then processed for cellular RNA extraction for amplification of p21, p27, and β-actin by RT-PCR.

treated with lovastatin [15]. In the present study, we showed that lovastatin-inhibited proliferation of ATC cells (ARO, 8305C, SW1736 and KAT4B) by increasing the level of p27 protein, which in turn inhibited the CDK2 activity, and ultimately arrested the cell cycle at the G1 phase. To our knowledge, this is the first demonstration that lovastatin inhibited the growth of human ATC cells through increases of the p27 protein.

Inhibition of the mevalonate pathway by lovastatin leads to blockade of the production of downstream isoprenoid-related compounds (such as FPP, GGPP, ubiquinone, dolichol, carotenoid, and squalene), which play important roles in numerous cellular biological functions [9,10]. As shown in Fig. 1C and D, the lovastatin-induced anti-proliferation and cell cycle arrest were completely prevented by mevalonate and partially by GGPP, suggesting that blockade of mevalonate production is responsible for the cell growth inhibition induced by lovastatin. On the other hand, FPP at a concentration of 30 μM did not affect the lovastatin-induced growth inhibition in ARO cells. In the presence of lovastatin, the apoptotic cell death was observed when the FPP concentration was higher than 30 μM (data not shown). These results suggested that a depletion of an intracellular GGPP reservoir was associated, at least in part, with lovastatin-induced growth inhibition in ARO cells. Since a lesser effect of GGPP (even at concentrations higher than 30 μM) on the prevention of lovastatin-induced antiproliferation was observed in comparing with of mevalonate, which is a direct downstream metabolite of HMG-CoA and an upstream intermediate of GGPP, it is possible that other isoprenoids (such as dolichol, ubiquinone, and carotenoid) might be also involved in the prevention of proliferation inhibition induced by lovastatin. This issue deserves further investigation.

The protein structures of Ras and Rho contain a CAAX box at the carboxyl-terminal [C, cysteine; A, aliphatic amino acid; X, methionine, serine, leucine, or glutamine]. In the process of post-translational modification, prenyl transferase catalyzes and transfers an isoprenyl group (from FPP and GGPP) to cysteine (of CAAX box) followed by cleavage of the three downstream amino acids (AAX), and finally causes palmitoylation of cysteine residues in the region nearby [11]. After prenylation (e.g. farnesylation or geranylgeranylation), small GTPase proteins are translocated to the plasma membrane in response to stimulation of growth factors or integrins [19]. Farnesylation of Ras and geranylgeranylation of Rho are essential for their activation on the membrane. In the present study, our results showed that post-translational modifications of Rho family proteins (e.g. RhoA and Rac1) were inhibited as evidenced by a reduction of their translocations from cytosol to plasma membrane in the lovastatin-treated ARO cells (Fig. 3A and B). On the other hand, the protein processing and membrane anchorage of Ras in ARO cells was not affected by lovastatin or isoprenoids such as FPP. Nevertheless, the isoprenyl processes of both Ras and Rho were observed in the lovastatin-treated HUVEC (Fig. 3B, lower panel), suggesting that the lack of Ras responsiveness to lovastatin in ARO cells was not due to technical problems.

The Rho/ROCK signal pathway has been suggested to be involved in the regulation of cancer cell motility [16,20] and angiogenic actions [21]. Activation of the ROCK signal pathway may also promote tumor cell proliferation. It has been reported that the ROCK-selective inhibitor, Y27632, inhibited growth of cancer cells [22,23] and vascular smooth muscle and endothelial cells [24]. In the present study, we demonstrated that both lovastatin treatment and transfection of the cells with DN-RhoA cDNA induced increases of the level of p27 protein (Fig. 6B) and blockade of the ROCK activity by Y-27632 resulted in an increase of p27 protein (Fig. 8A), which in turn caused growth inhibition (Fig. 8B) in ARO cells. Moreover, the GGPP-induced prevention of lovastatin-induced p27 induction and cell cycle arrest were also

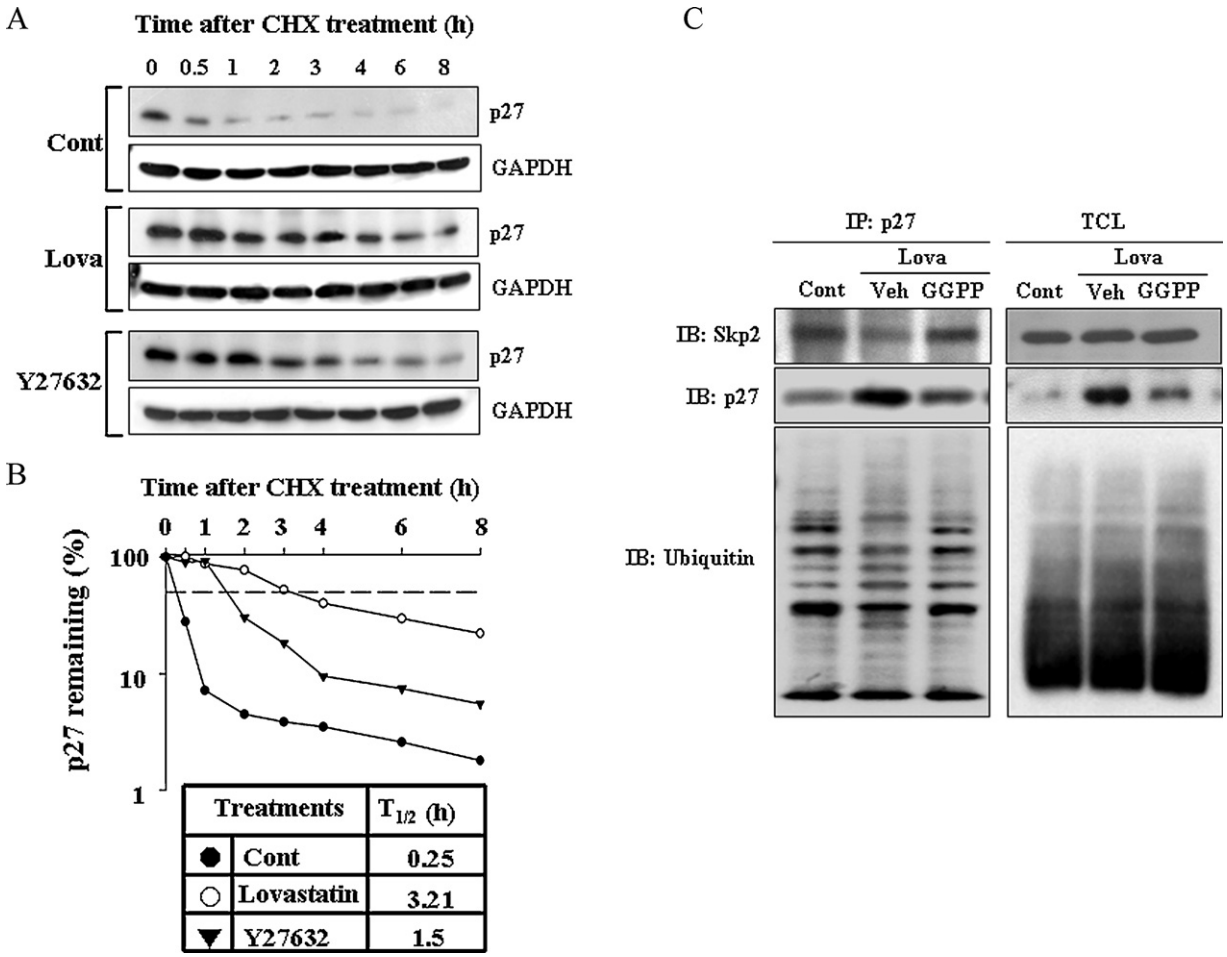

Fig. 7. Effects of ROCK and lovastatin on p27 protein stability. (A) Both lovastatin (20 μM) and Y27632 (2 μM) prevented the degradation of p27 protein in ARO cells. (B) The quantified results of p27 protein levels, which were adjusted with GAPDH protein level. The dotted line indicates 50% abundance of p27, and the half-life ($t_{1/2}$) of p27 protein in each group is shown in the lower panel. A representative result from three independent experiments is shown. ARO cells were cultured overnight and then treated with DMSO (Cont), lovastatin (Lova), or Y27632 for 40 h. Cells were subsequently treated with cycloheximide (CHX) for 0.5–8 h, and then harvested for cellular protein extraction at the indicated time points. The protein extracts were detected for p27 and GAPDH with specific antibodies. GAPDH blots were used as loading control. (C) Lovastatin inhibited the formation of p27–Skp2 complex and the levels of ubiquitinated p27-associated proteins. These effects were prevented by pretreatment of cells with GGPP. IP, immunoprecipitation; IB: immunoblotting; TCL, total cell lysate.

abolished by Y-27632. Interestingly, overexpression of constitutive RhoA did not prevent the lovastatin-induced increase of p27 protein (Fig. 6B). One possible explanation is that GGPP was depleted by lovastatin treatment and the RhoA is inactive in the absence of GGPP. Taken together, these results suggest that ROCK might keep the p27 protein at a low level, which led to the cell cycle progression and the aggressive proliferation of ARO cells.

HMG-CoA reductase inhibitors have been shown to induce G1 arrest in prostate [25], breast [26], and hepatic [27] cancer cells. Consistent with these findings, the results from the present study demonstrate that lovastatin arrested the cell cycle of ATC cells at the G1 phase. Previously, it has been reported that the level of p27 protein in ATC is low [28]. In the present study, our data suggest that an increase of the level of p27 protein is responsible for lovastatin-induced growth inhibition in ARO cells. The same findings were also observed in the other three ATC cell lines (8305C, SW1736 and KAT4B) except that the levels of p21 protein in 8305C, SW1736 and KAT4B were also increased (data not shown). Based on the results from the present study, we propose a model of the molecular mechanisms underlying lovastatin-induced cell cycle arrest in ARO cells as shown in Fig. 9.

Although our present study demonstrated that lovastatin-inhibited ARO cell proliferation *in vitro*, the effective concentrations of lovastatin used for induction of anti-proliferation in human patients need further investigation. The dose of lovastatin used for lowering serum cholesterol in human clinical treatment is about 0.25–1.0 mg/kg, B.W. In a phase I study, the plasma concentrations of lovastatin measured in cancer patients were also relatively low (0.1–3.9 μM) [29]. It has been indicated that 43% reduction in newly diagnosed colorectal cancer cases during a 5-year follow-up in patients with coronary artery disease taking pravastatin [30]. Pravastatin (40 mg/day) significantly doubled the median survival time for elderly hepatocellular carcinoma patients [31]. Significant clinical responses of anaplastic astrocytoma, glioblastoma multiforme, gastric adenocarcinoma to lovastatin treatments were reported for patients enrolled in phase I–II trials in patients with gastric cancer [32], colorectal cancer [33], melanoma [34], and small cell lung cancer [35]. Moreover, lovastatin treatment induced cellular differentiation in ARO cells (at a concentration of 10 μM or less for cultured cells). The myopathy and hepatotoxicity caused by statins treatment is seldom observed in clinical long-term therapy, suggesting that the use of lovastatin (even at a dose as high as 80 mg/day) for clinical therapeutic purpose in hypercholesterolemia is quite safe [36]. Taken together, it is most likely that statins at lower concentrations than those used in the present study may be effective. The effective doses of statins on cancer treatment might be reduced by combined treatment with statins and the well-established

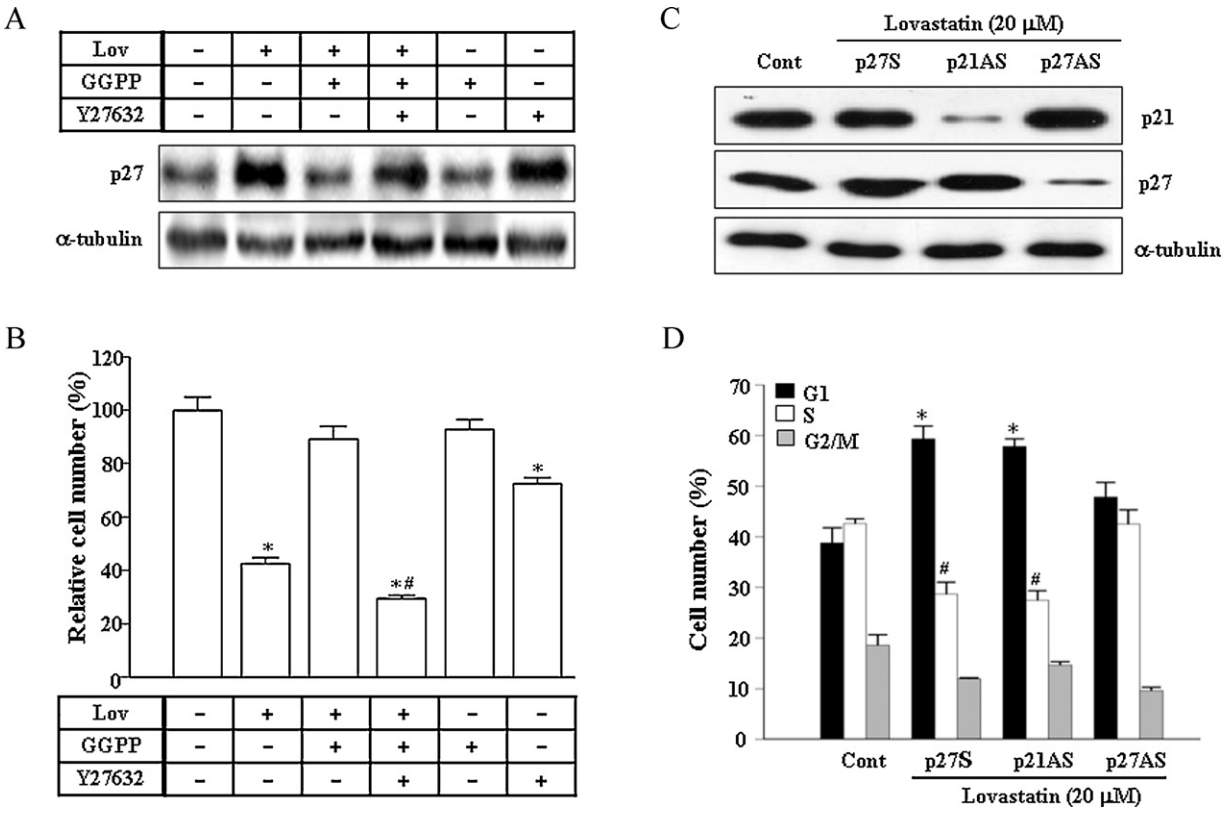

Fig. 8. Up-regulation of p27 is essential for cell cycle arrest induced by lovastatin. ARO cells were treated with lovastatin with or without GGPP (30 μM), Y27632 (2 μM), or GGPP (30 μM) + Y27632 (2 μM) for 48 h. The cells were then processed for protein extraction or cell number counting. Both lovastatin and Y27632 increased the level of p27 protein (A) and decreased the cell number (B) in ARO cells. Y27632 also abolished the GGPP-mediated prevention of lovastatin-induced growth inhibition in ARO cells. The growth of ARO cells was evaluated using MTT assay. Cell samples were analyzed in triplicate, and values represent the means ± S.E.M. Significance was accepted at $p < 0.05$. *Different from control group. #Different from lovastatin-treated group. The lovastatin-induced increases of p27 protein levels (C) and cell accumulation in the G1 phase were prevented by transfection of the cells with antisense p27 oligonucleotide (p27 AS), but not p21 AS or p27 scramble antisense (D). Western blot analyses were performed to examine the protein levels of p27 in ARO cells. Membrane was also probed with anti-α-tubulin antibody to verify equivalent loading. Antisense (p27AS or p21AS) or scramble antisense (p27S) oligonucleotide was transfected into ARO cells with liposome and incubated with lovastatin for additional 48 h. The cells were then collected for Western blot and cell cycle analysis. Cont, control; Veh, vehicle; AS, antisense; S, scramble AS. *Significant increase in G1 phase versus control group ($p < 0.05$). #Significant reduction in the S phase versus control group ($p < 0.05$).

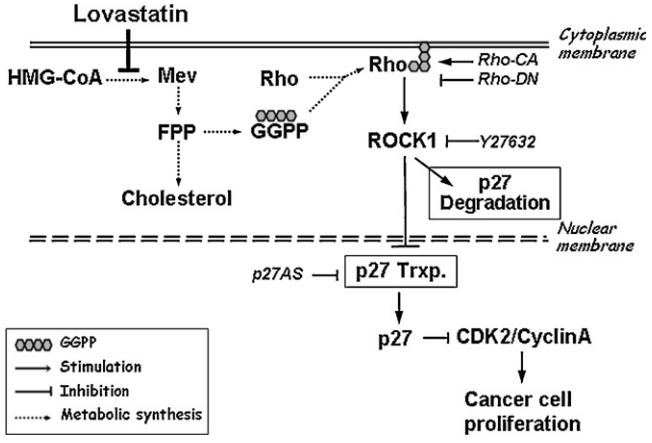

Fig. 9. Lovastatin reduces proliferation of anaplastic thyroid cancer cells. Treatment of ARO cells with lovastatin induces a Rho/ROCK-dependent increase of p27 protein level, which in turn inhibits the CDK2 activity, and finally causes cell cycle arrest at the G1 phase. In this study, RhoA-CA and RhoA-DN mutants were used to manipulate the activity of RhoA, whereas Y27632 was utilized to inhibit a direct activation of the RhoA/ROCK signaling pathway. Degrad., degradation; Trxp., transcription.

chemotherapeutic drugs [35]. Moreover, in addition to the anti-proliferation activity, lovastatin could induce the differentiation in the thyroid cancer cells, and thereafter, made them more sensitive to radioactive iodine therapy. In conclusion, the results from our previous and present studies strongly suggest the potential applications of lovastatin in the treatment of thyroid cancer.

Conflict of interest

The authors state no conflict of interest.

Acknowledgements

This work was supported by the National Science Council Grants NSC-100-2320-B-038-011 (WSL), NSC-95-2320-B-038-048 and NSC-97-2320-B-038-018-MY3 (WBZ).

References

[1] van Staveren WC, Solís DW, Delys L, Duprez L, Andry G, Franc B, et al. Human thyroid tumor cell lines derived from different tumor types present a common dedifferentiated phenotype. Cancer Res 2007;67:8113–20.
[2] Parameswaran R, Brooks S, Sadler GP. Molecular pathogenesis of follicular cell derived thyroid cancers. Int J Surg 2010;8:186–93.
[3] Mihailovic JM, Stefanovic LJ, Malesevic MD, Erak MD, Tesanovic DD. Metastatic differentiated thyroid carcinoma: clinical management and outcome of disease in patients with initial and late distant metastases. Nucl Med Commun 2009;30:558–64.
[4] Piccardo A, Arecco F, Morbelli S, Bianchi P, Barbera F, Finessi M, et al. Low thyroglobulin concentrations after thyroidectomy increase the prognostic value of undetectable thyroglobulin levels on levo-thyroxine suppressive treatment in low-risk differentiated thyroid cancer. J Endocrinol Invest 2010;33:83–7.
[5] Hong YJ, Jeong MH, Hachinohe D, Ahmed K, Choi YH, Cho SH, et al. Comparison of effects of rosuvastatin and atorvastatin on plaque regression in Korean patients with untreated intermediate coronary stenosis. Circ J 2011;75:398–406.

[6] Kawai Y, Sato-Ishida R, Motoyama A, Kajinami K. Place of pitavastatin in the statin armamentarium: promising evidence for a role in diabetes mellitus. Drug Des Devel Ther 2011;5:283–97.
[7] Sadowitz B, Maier KG, Gahtan V. Basic science review: statin therapy—Part I: the pleiotropic effects of statins in cardiovascular disease. Vasc Endovasc Surg 2010;44:241–51.
[8] Boudreau DM, Yu O, Johnson J. Statin use and cancer risk: a comprehensive review. Expert Opin Drug Saf 2010;9:603–21.
[9] Clendening JW, Pandyra A, Boutros PC, El Ghamrasni S, Khosravi F, Trentin GA, et al. Dysregulation of the mevalonate pathway promotes transformation. Proc Natl Acad Sci USA 2010;107:15051–6.
[10] Miziorko HM. Enzymes of the mevalonate pathway of isoprenoid biosynthesis. Arch Biochem Biophys 2011;505:131–43.
[11] Wright LP, Philips MR. Thematic review series: lipid posttranslational modifications. CAAX modification and membrane targeting of Ra. J Lipid Res 2006;47:883–91.
[12] Manandhar SP, Hildebrandt ER, Jacobsen WH, Santangelo GM, Schmidt WK. Chemical inhibition of CaaX protease activity disrupts yeast Ras localization. Yeast 2010;27:327–43.
[13] Vivaldi A, Miasaki FY, Ciampi R, Agate L, Collecchi P, Capodanno A, et al. Redifferentiation of thyroid carcinoma cell lines treated with 5-Aza-2′-deoxycytidine and retinoic acid. Mol Cell Endocrinol 2009;307:142–8.
[14] Zhong WB, Wang CY, Chang TC, Lee WS. Lovastatin induces apoptosis of anaplastic thyroid cancer cells via inhibition of protein geranylgeranylation and de novo protein synthesis. Endocrinology 2003;144:3852–9.
[15] Wang CY, Zhong WB, Chang TC, Lai SM, Tsai YF. Lovastatin, a 3-hydroxy-3-methylglutaryl coenzyme A reductase inhibitor, induces apoptosis and differentiation in human anaplastic thyroid carcinoma cells. J Clin Endocrinol Metab 2003;88:3021–6.
[16] Zhong WB, Liang YC, Wang CY, Chang TC, Lee WS. Lovastatin suppresses invasiveness of anaplastic thyroid cancer cells by inhibiting Rho geranylgeranylation and RhoA/ROCK signaling. Endocr Relat Cancer 2005;12:615–29.
[17] Gauthaman K, Fong CY, Bongso A. Statins, stem cells, and cancer. J Cell Biochem 2009;106:975–83.
[18] Fritz G. Targeting the mevalonate pathway for improved anticancer therapy. Curr Cancer Drug Targets 2009;9:626–38.
[19] ten Klooster JP, Hordijk PL. Targeting and localized signalling by small GTPases. Biol Cell 2007;99:1–12.
[20] Liu S, Goldstein RH, Scepansky EM, Rosenblatt M. Inhibition of rho-associated kinase signaling prevents breast cancer metastasis to human bone. Cancer Res 2009;69:8742–51.
[21] Bryan BA, Dennstedt E, Mitchell DC, Walshe TE, Noma K, Loureiro R, et al. RhoA/ROCK signaling is essential for multiple aspects of VEGF-mediated angiogenesis. FASEB J 2010;24:3186–95.
[22] Deng L, Li G, Li R, Liu Q, He Q, Zhang J. Rho-kinase inhibitor, fasudil, suppresses glioblastoma cell line progression in vitro and in vivo. Cancer Biol Ther 2010;9:875–84.
[23] Zhang S, Tang Q, Xu F, Xue Y, Zhen Z, Deng Y, et al. RhoA regulates G1-S progression of gastric cancer cells by modulation of multiple INK4 family tumor suppressors. Mol Cancer Res 2009;7:570–80.
[24] Harvey KA, Welch Z, Sliva D, Siddiqui RA. Role of Rho kinase in sphingosine 1-phosphate-mediated endothelial and smooth muscle cell migration and differentiation. Mol Cell Biochem 2010;342:7–19.
[25] Kochuparambil ST, Al-Husein B, Goc A, Soliman S, Somanath PR. Anticancer efficacy of simvastatin on prostate cancer cells and tumor xenografts is associated with inhibition of Akt and reduced prostate-specific antigen expression. J Pharmacol Exp Ther 2011;336:496–505.
[26] Ghosh-Choudhury N, Mandal CC, Ghosh-Choudhury N, Ghosh Choudhury G. Simvastatin induces derepression of PTEN expression via NFkappaB to inhibit breast cancer cell growth. Cell Signal 2010;22:749–58.
[27] Relja B, Meder F, Wilhelm K, Henrich D, Marzi I, Lehnert M. Simvastatin inhibits cell growth and induces apoptosis and G0/G1 cell cycle arrest in hepatic cancer cells. Int J Mol Med 2010;26:735–41.
[28] Tallini G, Garcia-Rostan G, Herrero A, Zelterman D, Viale G, Bosari S, et al. Downregulation of p27KIP1 and Ki67/Mib1 labeling index support the classification of thyroid carcinoma into prognostically relevant categories. Am J Surg Pathol 1999;23:678–85.
[29] Thibault A, Samid D, Tompkins AC, Figg WD, Cooper MR, Hohl R, et al. Phase I study of lovastatin, an inhibitor of the mevalonate pathway, in patients with cancer. Clin Cancer Res 1996;2:483–91.
[30] Friis S, Poulsen AH, Johnsen SP, McLaughlin JK, Fryzek JP, Dalton SO, et al. Cancer risk among statin users: a population-based cohort study. Int J Cancer 2005;114:643–7.
[31] Kawata S, Yamasaki E, Nagase T, Inui Y, Ito N, Matsuda Y, et al. Effect of pravastatin on survival in patients with advanced hepatocellular carcinoma. A randomized controlled trial. Br J Cancer 2001;84:886–91.
[32] Konings IR, van der Gaast A, van der Wijk LJ, de Jongh FE, Eskens FA, Sleijfer S. The addition of pravastatin to chemotherapy in advanced gastric carcinoma: a randomized phase II trail. Eur J Cancer 2010;46:3200–4.
[33] Lee J, Jung KH, Park YS, Ahn JB, Shin SJ, Im SA, et al. Simvastatin plus irinotecan, 5-fluorouracil, and leucovorin (FOLFIRI) as first-line chemotherapy in metastatic colorectal patients: a multicenter phase II study. Cancer Chemother Pharmacol 2009;64:657–63.
[34] Glynn SA, O'Sullivan D, Eustace AJ, Clynes M, O'Donovan N. The 3-hydroxy-3-methylglutaryl-coenzyme A reductase inhibitors, simvastatin, lovastatin and mevastatin inhibit proliferation and invasion of melanoma cells. BMC Cancer 2008;8:9.
[35] Han JY, Lim KY, Yu SY, Yun T, Kim HT, Lee JS. A phase 2 study of irinotecan, cisplatin, and simvastatin for untreated extensive-disease small cell lung cancer. Cancer 2010;117:2178–85.
[36] Davignon J, Hanefeld M, Nakaya N, Hunninghake DB, Insull Jr W, Ose L. Clinical efficacy and safety of cerivastatin: summary of pivotal phase IIb/III studies. Am J Cardiol 1998;82:32J–9J.